Research Square

Preprints are preliminary reports that have not undergone peer review.
They should not be considered conclusive, used to inform clinical practice,
or referenced by the media as validated information.

Flame Retardancy and Reinforcement–Toughening Mechanism of Epoxy Resin Modified with a Phosphorus–Nitrogen Synergistic Imidazolium Ionic Liquid

Yiru Kong
Shenyang University of Chemical Technology
Bing Liang
Shenyang University of Chemical Technology
Jiapeng Long
long2682@126.com

Shenyang University of Chemical Technology

Research Article

Keywords: Epoxy resin, imidazolium ionic liquid, phosphorus–nitrogen synergistic flame retardant, flame retardancy, char formation, mechanical properties

Posted Date: November 11th, 2026

DOI: https://doi.org/10.21203/rs.3.rs-11314870/v1

License: This work is licensed under a Creative Commons Attribution 4.0 International License.
Read Full License

Additional Declarations: No competing interests reported.

Flame Retardancy and Reinforcement–Toughening Mechanism of Epoxy Resin Modified with a Phosphorus–Nitrogen Synergistic Imidazolium Ionic Liquid

Yiru Kong[1], Bing Liang[1*], Jiapeng Long[1*]

[1] School of Material Science and Technology, Shenyang University of Chemical Technology, Shenyang 110142, People's Republic of China

Abstract

Epoxy resin (EP) is widely used in engineering applications, but it has inherent flammability issues, and balancing its flame retardancy with mechanical properties also poses challenges. In this study, a phosphorus and nitrogen-containing amide-functionalized imidazoline ionic liquid - 1-(carbamoylmethyl)-2-methylimidazolium dihydrogen phosphate ([CMMIm][H_2PO_4]) was synthesized, and it was introduced as a multifunctional flame retardant modifier into EP. Through LOI, TGA, cone calorimeter method, Raman spectroscopy, scanning electron microscope (SEM), and mechanical tests, the effects of [CMMIm][H_2PO_4] on flame retardancy, thermal degradation, carbonization formation and mechanical properties were systematically investigated. The addition of [CMMIm][H_2PO_4] significantly improved the fire resistance of EP. The LOI value of EP-4 increased from 20.41% to 30.68%, while the PHRR value decreased from 923.43 $kW \cdot m^{-2}$ to 563.61 $kW \cdot m^{-2}$, a reduction of approximately 39%. At 800°C, the carbonized residue content increased from 11.64% to 16.90%, and the ID/IG ratio decreased from 0.85 to 0.78, indicating a more stable carbonization structure. Meanwhile, EP-4 exhibited tensile strength of 73.91 MPa, bending modulus of 3522.38 MPa and impact strength of 16.75 $kJ \cdot m^{-2}$. These results indicate that [CMMIm][H_2PO_4] is an effective strategy that can enhance the flame

Corresponding author 1: Jiapeng Long, Email: long2682@126.com

Corresponding author 2: Bing Liang, Email: lb1007@163.com

retardancy of epoxy resin while improving its mechanical properties.

Keywords： Epoxy resin; imidazolium ionic liquid; phosphorus–nitrogen synergistic flame retardant; flame retardancy; char formation; mechanical properties

1. Introduction

Epoxy resin (EP) is one of the most widely used thermosetting polymers due to its excellent adhesion, chemical resistance, electrical insulation, dimensional stability, and mechanical strength[1-5]. These advantages have enabled its extensive application in electronic encapsulation, coatings, aerospace structures, transportation, and fiber-reinforced composites[6]. However, conventional EP is inherently flammable and releases considerable heat and combustible volatile products during combustion, which restricts its application in fields requiring high fire safety standards[2-4]. Therefore, developing flame-retardant EP systems while maintaining mechanical performance remains an important research challenge.

Halogen-free phosphorus- and nitrogen-containing flame retardants have attracted significant attention as alternatives to traditional halogenated systems. Phosphorus-containing compounds can promote dehydration, crosslinking, and char formation in the condensed phase, and may also inhibit flame propagation through gas-phase radical scavenging mechanisms. Meanwhile, nitrogen-containing structures can contribute to char stabilization and synergistic flame-retardant effects[4,7,25]. However, conventional additive flame retardants often require relatively high loading levels to achieve satisfactory flame retardancy, which may lead to poor dispersion, phase separation, weakened interfacial interactions, and reduced mechanical properties of EP. Therefore, multifunctional flame retardants capable of simultaneously improving fire safety and mechanical performance have attracted increasing research interest[10,14,19].

Ionic liquids (ILs) have emerged as promising platforms for designing multifunctional flame retardants because their cationic and anionic structures can be independently tailored. Among them, imidazolium-based ILs are particularly attractive due to their nitrogen-containing heterocyclic structures and strong interactions with polymer networks. By introducing phosphorus-containing anions or phosphorus-

functionalized groups, ILs can integrate phosphorus and nitrogen elements into a single molecular system, providing an effective approach for flame-retardant modification of epoxy resin[8-16]. Previous studies have demonstrated that phosphorus-containing imidazolium ILs can reduce heat release, promote char formation, and improve the comprehensive properties of EP systems[9,12,15,16].

Several phosphorus-containing ionic liquid systems have been reported for flame-retardant epoxy modification. Shi et al.[9] developed the phosphorus-containing halogen-free ionic liquid [Dmim]Tos, which increased the LOI value of EP to 32.5% at a loading of 4 wt.% and reduced the PHRR by approximately 37%, although a plasticizing effect was observed. Wei et al.[17] reported DOPA-MZ, which achieved an LOI value of 30.3% at only 3 wt.% loading while improving the tensile and flexural properties of EP. Xiao et al.[18] developed BDBP, which increased the LOI value to 31.9% and reduced PHRR by 48.1%. More recently, phosphorus-containing imidazolium systems, such as [Mim]TBP and DOPO-derived ionic liquids, have shown promising improvements in flame retardancy, toughness, and mechanical performance[20-24]. Nevertheless, some reported systems rely on complex molecular structures, multistep synthesis procedures, or relatively high additive contents. Thus, developing flame retardants with simple structures, efficient flame-retardant performance, and mechanical reinforcement remains challenging.

As summarized in Table 1, phosphorus-containing ionic liquids generally provide effective flame-retardant performance for EP, with LOI values above 30% and considerable reductions in PHRR being achieved in several reported systems. Some ionic liquids also improve the mechanical properties of EP, although performance trade-offs or relatively high additive loadings are observed in certain cases. In comparison, the [CMMIm][H_2PO_4]/EP system developed in this work achieves an LOI of 30.68% and a 39% reduction in PHRR at a loading of 5.67 wt.%, together with increases of 26%, 40%, and 86% in tensile strength, flexural modulus, and impact strength, respectively. These results indicate a favorable balance between flame retardancy and mechanical performance.

In this work, an amide-functionalized phosphorus–nitrogen-containing

imidazolium ionic liquid, [CMMIm][H_2PO_4], was designed and synthesized for epoxy modification. The ionic liquid was prepared through quaternization of 2-methylimidazole with chloroacetamide, followed by anion exchange with sodium dihydrogen phosphate. Compared with previously reported phosphorus-containing ionic liquids with complex aromatic structures, [CMMIm][H_2PO_4] possesses a relatively simple molecular structure and can be synthesized using readily available raw materials. The $H_2PO_4^-$ anion is expected to promote dehydration and catalytic carbonization during thermal degradation, while the imidazolium and amide groups provide nitrogen-containing functionalities and polar interaction sites with the epoxy network.

The influence of [CMMIm][H_2PO_4] on the flame retardancy, thermal degradation behavior, char structure, and mechanical properties of EP was systematically investigated. The relationship between ionic liquid incorporation, protective char formation, and mechanical reinforcement was further analyzed, providing a practical strategy for developing multifunctional flame-retardant epoxy materials.

Table 1 Comparison with studies on flame-retardant epoxy resins containing phosphorus-based ionic liquids

flame-retardant system	addition amount	LOI	PHRR	Mechanical properties	Re
[Dmim]Tos/EP	4wt.%	32.5%	↓37%	Modulus ↑ Impact ↓	[9]
DOPA-MZ/EP	3wt.%	30.3%	/	Tensile ↑ 22% Modulus ↑ 17%	[17]
BDBP/EP	4wt.%	31.9%	↓ 48.1%	Tensile ↑ 7%	[18]
[Mim]TBP/EP	≥10phr	>30%	↓ 31.5%	Tensile ↑ 100.2% Modulus ↑ 71.7% Impact ↑ 58.3%	[20]
[CMMlm][H_2PO_4]/EP	5.67wt.%	30.68%	↓ 39%	Tensile ↑ 26% Modulus ↑ 37%	/

	Impact ↑ 86%

2. Experimental

2.1 Experimental Materials

2-Methylimidazole (2-MI), chloroacetamide (CAA), sodium dihydrogen phosphate (NaH_2PO_4), and bisphenol-A epoxy resin (E-51) were supplied by Shanghai Macklin Biochemical Co., Ltd. (Shanghai, China). Acetonitrile and 4,4-diaminodiphenylmethane (DDM) were purchased from Sinopharm Chemical Reagent Co., Ltd. (Shanghai, China).

2.2 Preparation of Ionic Liquid [CMMIm][H_2PO_4]

First, 8.21 g of 2-MI was placed in a three-necked flask and dissolved in 150 mL of anhydrous acetonitrile. Separately, 9.351 g of CAA was dissolved in 100 mL of anhydrous acetonitrile, and the resulting solution was transferred to a dropping funnel. The CAA solution was then added dropwise to the 2-MI solution over approximately 30 min. The reaction mixture was magnetically stirred at 75 °C in an oil bath under a nitrogen atmosphere, with a condenser and a tail-gas absorption device connected to the reaction system. The molar ratio of 2-MI to CAA was 1:1. After completion of the dropwise addition, the reaction was maintained at 75 °C for 6 h. The mixture was subsequently cooled to room temperature, filtered under reduced pressure, and dried at 70 °C to obtain the white powdered intermediate, 1-(carbamoylmethyl)-2-methylimidazolium chloride ([CMMIm]Cl).

For the anion-exchange reaction, 0.6958 g of [CMMIm]Cl and 0.7805 g of NaH_2PO_4 were placed in a three-necked flask containing 30 mL of distilled water. The mixture was reacted at 80 °C for 24 h. After completion of the reaction, the mixture was dried at 100 °C to obtain pale-yellow liquid [CMMIm][H_2PO_4]. The synthetic route of [CMMIm][H_2PO_4] is shown in Figure 1.

2.3 Preparation of Epoxy Resin Composites

Different amounts of [CMMIm][H_2PO_4] were then incorporated into the epoxy resin and continuously stirred at 60 °C. DDM was melted at 100 °C before being added

to the mixture. After thorough mixing, trapped air bubbles were removed under vacuum. The resulting mixture was poured into a polytetrafluoroethylene mold and cured through a stepwise heating procedure at 80, 120, and 150 °C for 2 h at each temperature. After curing, the samples were allowed to cool slowly to room temperature. The contents of [CMMIm][H_2PO_4] in the prepared systems were 0.80%, 2.41%, 4.03%, and 5.67%, respectively. The formulations of the neat and flame-retardant epoxy samples are listed in Table 2..

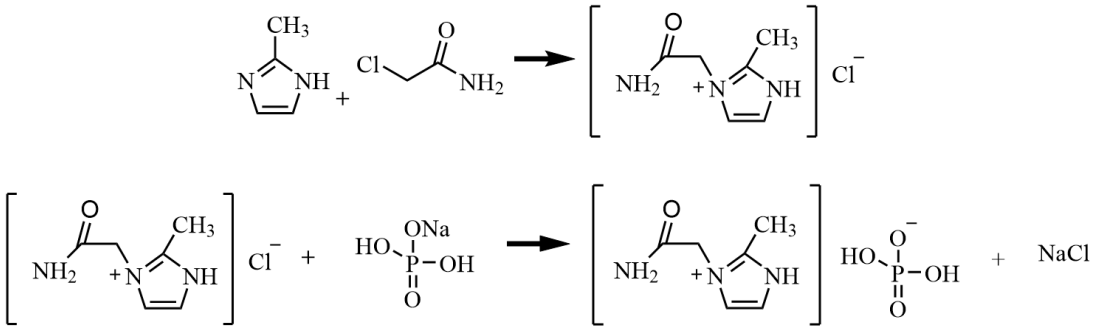


Figure 1 Synthetic route of [CMMIm][H_2PO_4]

Table 2 The preparation of EP and epoxy resin composites samples

Samples	EP/g	IL/g	DDM/g	P(wt/%)
EP-0	100	0	25.24	0
EP-1	100	1	23.98	0.105
EP-2	100	3	21.45	0.315
EP-3	100	5	18.93	0.527
EP-4	100	7	16.41	0.741

Calculation of phosphorus content P(wt%): P(wt%) = (mass of [CMMIm][H_2PO_4] / total mass of the system) × x × 100, where x is the mass fraction of P in [CMMIm][H_2PO_4].

2.4 Testing and Characterization

Fourier-transform infrared spectroscopy (FTIR): The functional groups of 2-MI, [CMMIm]Cl, and [CMMIm][H_2PO_4] were characterized using a Nexus-470 Fourier-transform infrared spectrometer (Thermo Fisher Scientific, USA). The spectra were collected over the range of 600–4000 cm^{-1} at a resolution of 1 cm^{-1}.

Nuclear magnetic resonance spectroscopy (NMR): The molecular structure of [CMMIm][H_2PO_4] was characterized at room temperature using a 500 MHz NMR

spectrometer (Bruker, Germany), with DMSO-d_6 or D_2O as the solvent.

High-resolution mass spectrometry (HRMS): HRMS characterization was performed using an Agilent 6550 QTOF high-resolution mass spectrometer (Agilent, USA) equipped with an electrospray ionization (ESI) source. Methanol was used as the solvent, and measurements were conducted in positive-ion mode.

Thermogravimetric analysis (TGA): The thermal stability of the samples was evaluated using an STA-449 C simultaneous thermal analyzer (Netzsch, Germany). Under a nitrogen atmosphere, the samples were heated from room temperature to 800 °C at a heating rate of 10 °C·min^{-1}.

UL-94 vertical burning test: The UL-94 test was performed using a CZF-3 testing instrument (Nanjing Jiangning Instrument Factory, China). The dimensions of the specimens were 130.0 × 9.5 × 4.0 mm^3.

Limiting oxygen index (LOI): LOI measurements were carried out using a JF-3 oxygen index instrument (Nanjing Jiangning Instrument Factory, China) in accordance with GB/T 2406-93. The specimen dimensions were 130.0 × 9.5 × 4.0 mm^3. Five specimens were tested for each group, with a sample mass deviation of ±0.3 g. Limiting oxygen index is calculated according to Formula (1):

$$LOI = \frac{[O_2]}{[N_2]+[O_2]} \times 100\% \qquad (1)$$

Cone calorimetry (CONE): Cone calorimeter measurements were conducted using an FTT 0007 cone calorimeter (FTT, UK) according to ISO 5660-1. The specimen dimensions were 100.0 × 100.0 × 3.0 mm^3, and an external heat flux of 50 kW·m^{-2} was applied.

Scanning electron microscopy (SEM): The morphology of the char residues after combustion was examined using a JSM-6360 LV scanning electron microscope (JEOL, Japan). All samples were sputter-coated with gold prior to observation.

Dynamic mechanical analysis (DMA): The dynamic thermomechanical properties of the [CMMIm][H_2PO_4]/EP composites were evaluated using a TA Q800 dynamic mechanical analyzer (TA Instruments). The specimens were tested in three-point bending mode at a frequency of 1 Hz under a nitrogen atmosphere. The temperature

was increased from 30 to 250 °C at a heating rate of 3 °C·min^{-1}. The storage modulus and loss factor (tan δ) were recorded as functions of temperature, and the glass-transition temperature (Tg) was determined from the peak position of the tan δ curve.

Raman spectroscopy: The char residues obtained after combustion were characterized using a Lab RAM HR confocal Raman spectrometer (HORIBA Scientific, France).

Mechanical property tests: Tensile properties were measured according to GB/T 2567-2008 using a TCS-2000 microcomputer-controlled electronic universal testing machine (China Gaotie Technology Co., Ltd.) at a crosshead speed of 2 mm·min^{-1}. Flexural tests were conducted according to GB/T 2567-2021 at a loading speed of 2 mm·min^{-1}. Impact strength was determined using a GT-704-MDL digital impact tester (China Gaotie Technology Co., Ltd.) in accordance with GB/T 2567-2021, using a simply supported beam configuration with a 2 kJ pendulum.

3.Results and Discussion

3.1 FTIR Characterization of [CMMIm][H_2PO_4]

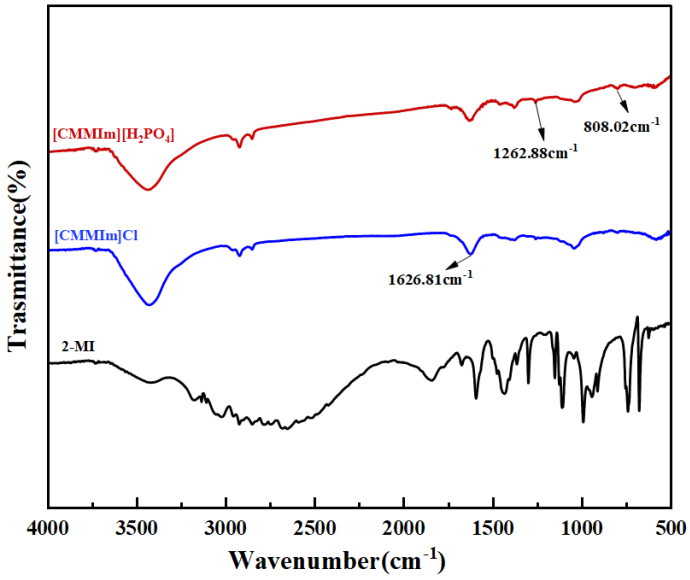


Figure. 2 FTIR spectra of [CMMIm][H_2PO_4]

Figure 2 presents the FTIR spectra of 2-MI, [CMMIm]Cl, and [CMMIm][H_2PO_4]. The spectrum of 2-MI mainly exhibits characteristic absorption bands associated with the imidazole ring. After reaction with chloroacetamide, [CMMIm]Cl shows a new

absorption peak at 1626.81 cm^{-1}, which is assigned to the stretching vibration of the amide carbonyl group (C=O). The appearance of this peak confirms the introduction of the carbamoylmethyl group through the N-alkylation reaction between 2-MI and CAA, resulting in the formation of the imidazolium chloride intermediate.

After the anion-exchange reaction, the characteristic C=O absorption peak at 1626.81 cm^{-1} remains unchanged in the spectrum of [CMMIm][H_2PO_4], indicating that the cationic structure and amide functionality are preserved during the exchange process. Meanwhile, two new absorption bands appear at 1262.88 and 808.02 cm^{-1}, corresponding to phosphate-related vibrations. The peak at 1262.88 cm^{-1} is attributed to the P=O stretching vibration, while the band near 808.02 cm^{-1} is assigned to P–O vibration. The emergence of these characteristic phosphate peaks confirms the successful introduction of the $H_2PO_4^-$ component into the ionic liquid structure.

Therefore, the FTIR results verify the successful construction of the imidazolium-based ionic liquid containing amide and phosphate functional groups.

3.2 NMR Spectroscopic Analysis of [CMMIm][H_2PO_4]

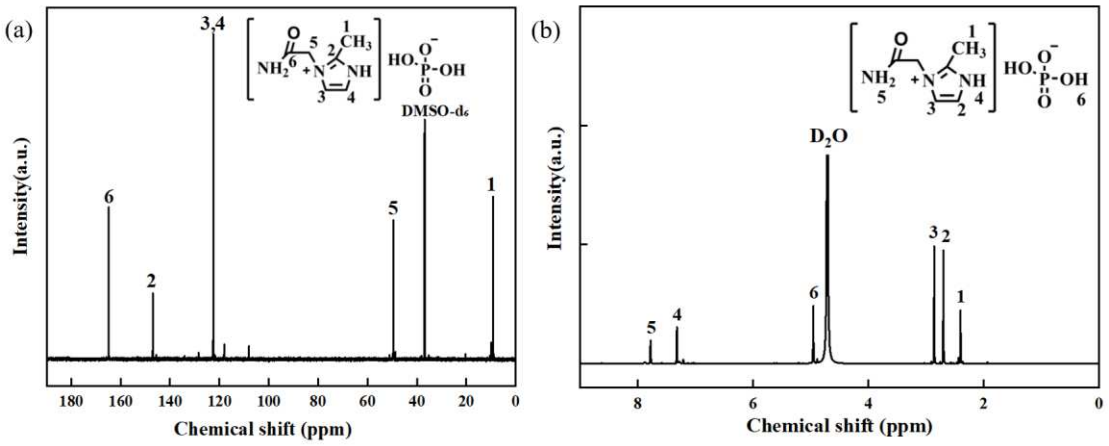


Figure 3 NMR spectrum of [CMMIm][H_2PO_4] a) ^{13}C-NMR; b) ^{1}H-NMR

The structure of the synthesized ionic liquid was characterized by ^{13}C NMR and ^{1}H NMR, and the spectra are shown in Figures 3. In Figure 3 (a), the strong peak near δ=39 ppm originates from the solvent peak of DMSO-d_6 used in the test. A distinct carbonyl carbon signal of the product appears at δ=165 ppm, which can be assigned to the C=O in the side-chain amide group –$CONH_2$; the signal at δ=145 ppm is attributed to the C2 carbon of the imidazole ring linked to the methyl group at position 2.

Characteristic signals for the two unsaturated carbons C3 and C4 on the imidazole ring emerge near δ=122 ppm. Owing to their similar chemical environments, they possess close chemical shifts and appear as overlapping or nearly overlapping strong signals in the spectrum. In addition, a characteristic signal for the methylene carbon in the side-chain $N^+–CH_2–CONH_2$ is observed at δ=50 ppm. The presence of this signal indicates that the chlorine atom in chloroacetamide is substituted by the nitrogen atom of the imidazole ring, forming the N–CH_2 bond between imidazolium nitrogen and methylene, which demonstrates that chloroacetamide has been successfully grafted onto 2-methylimidazole. The signal at δ=9 ppm is assigned to the methyl carbon –CH_3 at position 2 of the imidazole ring. In summary, characteristic signals including methyl carbon of the imidazole ring, unsaturated carbons of the imidazole ring, N–CH_2 methylene carbon and amide carbonyl carbon are observed in the ^{13}C NMR spectrum. All major carbon signals are consistent with the expected structure of the target imidazolium cation, confirming that the chloroacetamide moiety has been successfully introduced into the 2-methylimidazole framework to form the desired organic cation structure.

In Figure 3 (b), the signal at δ = 2.4 ppm is assigned to the protons of the 2-position methyl CH_3 on the imidazole ring; the signals at δ = 2.7 and 2.8 ppm are assigned to the imidazole ring H, respectively. The signal peak at approximately δ = 4.7 ppm in the spectrum originates from the D_2O solvent. The signal at δ = 4.9 ppm is assigned to P–OH in $H_2PO_4^-$. δ = 7.3 is assigned to the methylene group $N^+–CH_2–CONH_2$ linked to the imidazolium nitrogen. The appearance of this characteristic signal indicates that the chloroacetamide group has been successfully attached to the nitrogen atom of the imidazole ring, and the signal at 7.7 ppm is assigned to the amide –NH_2. This demonstrates the formation of the imidazolium ionic liquid structure.

3.3 Mass Spectrometry Analysis of [CMMIm][H_2PO_4]

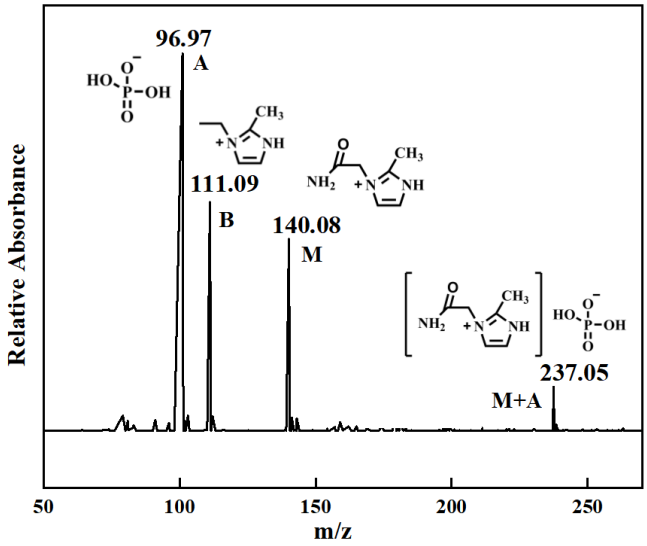


Figure. 4 Mass spectra of [CMMIm][H_2PO_4]

Table 3 Mass-to-charge ratios of different fragments

mass spectrum fragments	M	A	B	[M+A]
molecular weight	140.08	96.97	111.09	237.05
molecular formula	$C_6H_{10}N_3O^+$	$H_2O_4P^-$	$C_6H_{11}N_2^+$	$C_6H_{12}N_3O_5P$

High-resolution mass spectrometry was employed to further verify the molecular composition of the synthesized ionic liquid. The characteristic mass signals observed in the HRMS spectrum correspond well with the expected molecular fragments of [CMMIm][H_2PO_4].

The detected ions confirm the presence of the imidazolium-based cationic structure and phosphate-containing species. Together with FTIR and NMR characterization, the HRMS results support the successful preparation of the phosphorus- and nitrogen-containing ionic liquid.

3.4 Thermogravimetric Analysis of Epoxy Resin Composites

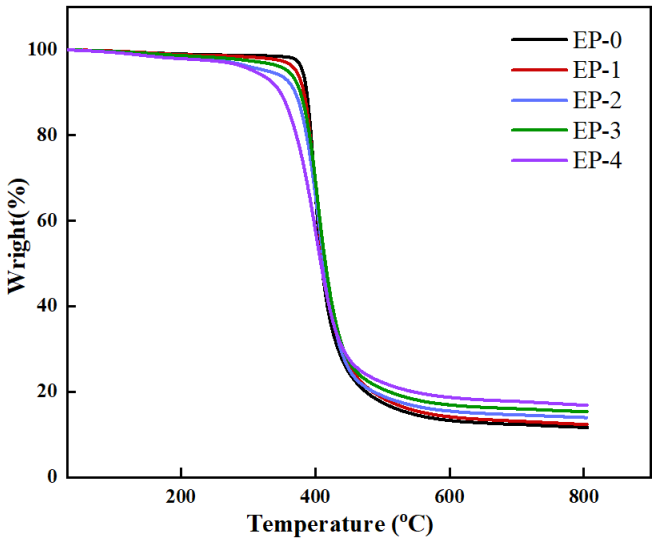


Figure. 5 Thermogravimetric curve of epoxy resin composites

Table 4 TG parameters of epoxy resin composites under N_2 conditions

Samples	$T_{5\%}$(℃)	T_{max}(℃)	R_{800}(%)
EP-0	383.53	376.28	11.64
EP-1	374.49	367.44	12.45
EP-2	362.38	362.47	14.00
EP-3	337.82	358.93	15.38
EP-4	302.47	338.82	16.90

TG tests were performed to evaluate the effect of [CMMIm][H_2PO_4] dosage on the thermal stability of epoxy resin. Figure 5 and Table 4 present the relevant data results. Thermogravimetric analysis results show that EP-0 to EP-4 all undergo rapid thermal decomposition mainly in the range of approximately 350-450 °C. With the increase of ionic liquid content, the initial thermal decomposition temperature of the modified epoxy resin decreases to a certain extent. Samples with high loading exhibit an obvious advanced weight loss phenomenon, indicating that the phosphorus-containing ionic liquid can promote dehydration and carbonization reactions of the matrix at relatively low temperatures. Meanwhile, the char yield of each modified system at high temperatures is higher than that of unmodified EP-0 and gradually rises as the ionic liquid content increases. At 800 °C, the char yield of EP-0 is 11.64%, while

that of EP-4 increases to approximately 16.90%. This demonstrates that the introduced ionic liquid can effectively promote the condensed-phase carbonization process of epoxy resin. Its phosphorus-containing components can form phosphoric acid species with dehydration catalytic effects during thermal decomposition, facilitating cross-linking and carbonization of the matrix and forming a relatively stable char layer, thereby improving the high-temperature char yield of the material.

3.5 Flame Retardancy Analysis of Epoxy Resin Composites

Table 5 LOI and UL-94 vertical burning results of samples with different compositions

Samples	LOI(%)	UL-94	t_1(s)	t_2(s)	Dripping
EP-0	20.41	Burn	＞30	——	Yes
EP-1	25.78	V-1	17.56	15.11	No
EP-2	27.38	V-1	14.84	12.88	No
EP-3	28.55	V-1	12.28	10.82	No
EP-4	30.68	V-0	5.52	3.85	No

The flame-retardant properties of the epoxy resin composites were evaluated by limiting oxygen index (LOI) and UL-94 vertical burning tests, and the results are summarized in Table 5. Neat EP-0 exhibits an LOI of 20.41%, suggesting that it is readily combustible under relatively low oxygen concentrations. The incorporation of [CMMIm][H_2PO_4] leads to a progressive increase in LOI. Specifically, the value increases to 25.78% for EP-1, followed by 27.38% and 28.55% for EP-2 and EP-3, respectively. EP-4 shows the highest LOI of 30.68%, approximately 50% higher than that of EP-0. These results indicate that a higher oxygen concentration is required to sustain combustion after the addition of [CMMIm][H_2PO_4], reflecting the reduced flammability of the modified epoxy resin.

The improvement in LOI is likely related to the phosphorus-containing species in [CMMIm][H_2PO_4]. During heating, these species can promote dehydration and char formation of the epoxy matrix, producing a protective carbonaceous layer that limits heat transfer and the release of combustible volatiles. In addition, the nitrogen-containing imidazolium structure may act synergistically with the phosphorus species during combustion. As a result, increasing the [CMMIm][H_2PO_4] content enhances the

resistance of the epoxy system to sustained burning.

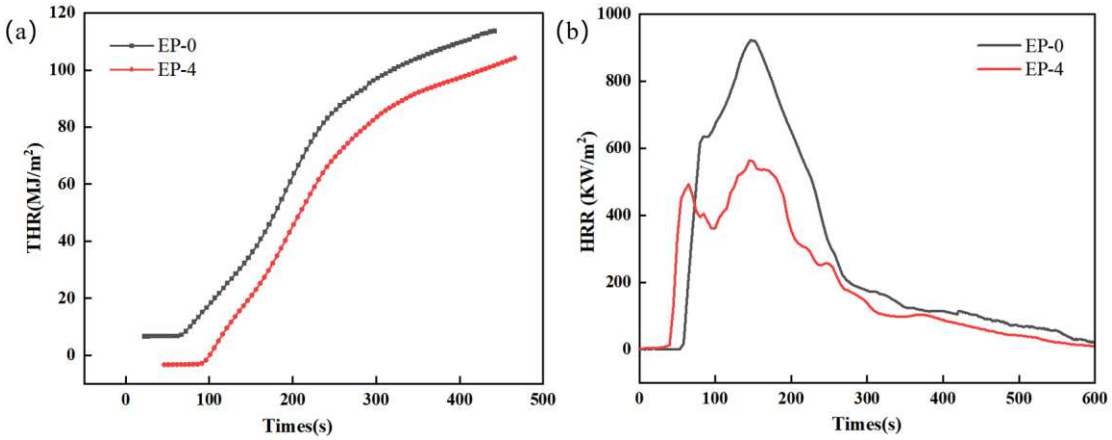


Figure. 6 Cone calorimetric test analysis a) TRR curves of epoxy resin composites b) HRR curves of epoxy resin composites

Table 6 CCT results of samples with different compositions

Samples	PHRR (kW/m^2)	THR (MJ/m^2)
EP-0	923.43	113.38
EP-4	563.61	104.37

PHRR represents the maximum heat release rate per unit area during combustion and is commonly used to characterize the intensity of heat release. THR refers to the cumulative heat released per unit area over the entire test period and provides an indication of the overall heat output of a material.

Cone calorimetry was further employed to investigate the combustion behavior of the epoxy resin composites, with the results presented in Figure 6 and Table 6. The incorporation of [CMMIm][H_2PO_4] noticeably reduces the heat release of epoxy resin during combustion. Neat EP-0 exhibits a PHRR of 923.43 $kW \cdot m^{-2}$, whereas the value decreases to 563.61 $kW \cdot m^{-2}$ for EP-4, corresponding to a reduction of approximately 39%. This substantial decrease indicates that the maximum heat release intensity is effectively suppressed by the ionic liquid. A similar, although less pronounced, change is observed in THR. The final THR decreases from 113.38 $MJ \cdot m^{-2}$ for EP-0 to 104.37 $MJ \cdot m^{-2}$ for EP-4, representing a reduction of 7.95%.

Compared with EP-0, the heat release rate (HRR) curve of EP-4 is lower, and the

heat release process is less concentrated. The main heat release is distributed over multiple stages rather than a single intense event. This behavior is consistent with the carbonization tendency observed in thermogravimetric analysis. During the combustion process, the phosphorus-containing species produced by [[CMMIm][H_2PO_4]] may promote the gel phase reaction and facilitate the formation of a protective carbon layer. This carbon layer can hinder heat transfer and limit the escape of combustible degradation products, thereby slowing down the further combustion of the epoxy resin matrix. The reduction of PHRR and THR is consistent with the improving trend in the LOI measurement results, supporting the positive role of [CMMIm][H_2PO_4] in reducing the combustion intensity of the epoxy resin.

3.6 Flame-retardant Mechanism Diagram of Epoxy Resin Composites

The flame-retardant effect of phosphorus- and nitrogen-containing imidazoline ionic liquids on epoxy resins is mainly attributed to gel-phase carbonization, and may also be influenced by free radical quenching in the gas phase. As shown in Figure 7, during the thermal decomposition process, $H_2PO_4^-$ can generate phosphoric acid, polyphosphoric acid, and related phosphorus compounds. These products promote the dehydration and cross-linking of the epoxy matrix, facilitating the formation of protective carbon layers. The formed carbonaceous layer acts as a physical barrier, restricting the transfer of heat and oxygen, and simultaneously inhibiting the release of flammable degradation products, thereby suppressing the further decomposition and combustion of the underlying matrix.

The nitrogen-containing structures in the imidazoline ring and the amide group may also be involved in the formation of char residue and interact with the phosphorus species, enhancing the stability of the residual char through a possible P-N synergistic effect. In the gas phase, the phosphorus-containing fragments generated during the decomposition process can absorb highly reactive H· and OH· radicals, thereby interfering with the chain reaction of flame spread. The combined effect of these processes explains why the modified epoxy system exhibits lower heat release, higher char residue content, and higher LOI. Overall, [CMMIm][H_2PO_4] mainly promotes the gel state protection, and may also provide additional flame retardant effects in the gas

phase.

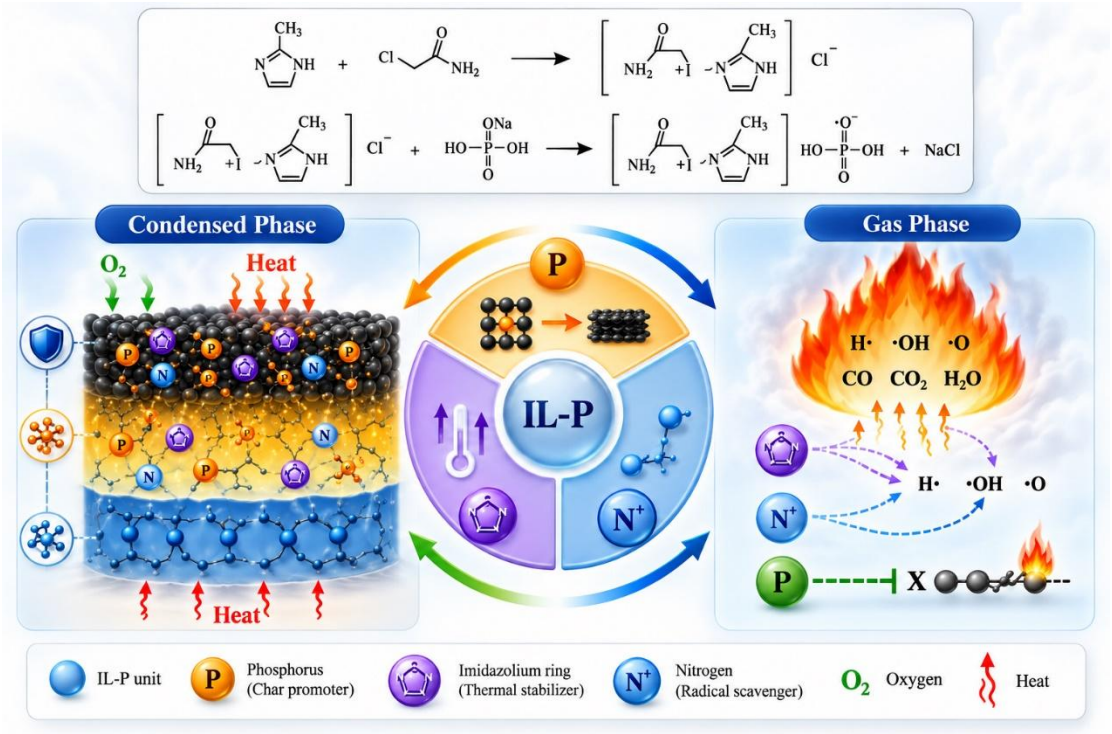


Figure 7 Flame-retardant mechanism diagram of epoxy resin composites

3.7 Scanning Electron Microscopy Analysis of Combustion Residue of Epoxy Resin Composites

SEM was used to examine the morphology of the char residues and evaluate the influence of [CMMIm][H_2PO_4] on char formation during combustion. As shown in Figure 8, the char residue of neat EP-0 has a loose and discontinuous surface with numerous large pores, indicating poor structural integrity. Such a porous structure would provide only limited protection against heat transfer and the release of combustible degradation products.

After the incorporation of [CMMIm][H_2PO_4], the morphology of the char residue changes noticeably. EP-1 develops a more continuous surface with fewer large pores, suggesting improved char formation. For EP-2, lamellar and wrinkled features become more apparent, accompanied by a further improvement in the continuity of the carbonaceous layer. At a higher [CMMIm][H_2PO_4] loading, EP-4 exhibits a relatively compact and continuous char surface with pronounced rough and aggregated features, while large pores are substantially reduced. The improved integrity of the residue is expected to strengthen its barrier effect by restricting heat and mass transfer between

the condensed and gas phases.

The progressive change from a loose and porous residue to a more compact and continuous char layer is consistent with the char-promoting effect of [CMMIm][H_2PO_4]. Phosphorus-containing species generated during thermal decomposition may facilitate dehydration and cross-linking reactions of the epoxy matrix, thereby promoting char formation. Nitrogen-containing groups in the ionic liquid may also contribute to this process through P–N interactions. Together with the Raman results, the SEM observations suggest that [CMMIm][H_2PO_4] improves both the structural integrity and carbon ordering of the residual char, providing further support for its condensed-phase flame-retardant action.

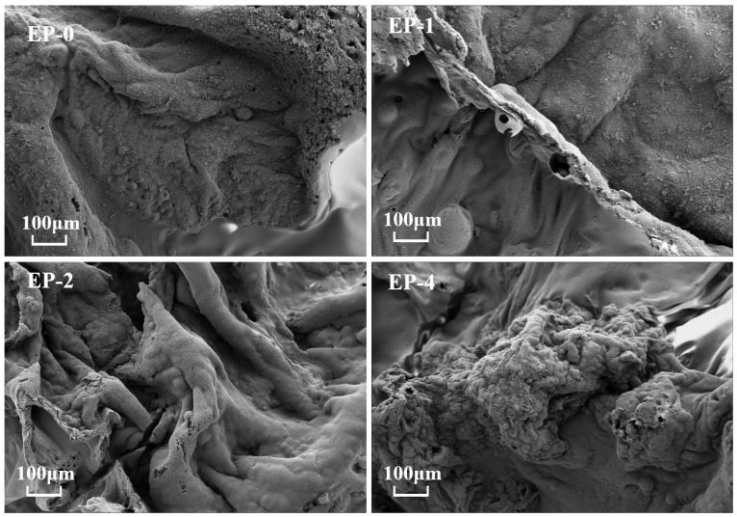


Figure. 8 SEM images of epoxy resin composites

3.9 Raman Analysis of Residual Char of Epoxy Resin Composites

The carbon structure of the combustion residue was analyzed by Raman spectroscopy. As shown in Figure 9, EP-0 and EP-4 exhibited two characteristic peaks at approximately 1350 cm^{-1} and 1580 cm^{-1}, respectively, corresponding to the D band and the G band. The D band is related to defects and disordered carbon structures, while the G band is associated with the vibration of sp^2 hybridized carbon atoms in the plane. The ratio of the intensities of these two peaks (I_D/I_G) is often used to evaluate the structural order of the carbonaceous residue. The lower the value, the higher the degree of graphitization.

The I_D/I_G ratio decreases from 0.85 for EP-0 to 0.78 for EP-4, suggesting that the

char formed by EP-4 contains a relatively more ordered carbon structure. This change indicates that the incorporation of [CMMIm][H_2PO_4] favors the formation of a more graphitized carbonaceous residue during combustion. Such a char structure is expected to provide a more effective protective barrier, helping to restrict heat transfer and the release of combustible degradation products. The Raman results therefore support the condensed-phase flame-retardant mechanism proposed for the [CMMIm][H2PO4]/EP system.

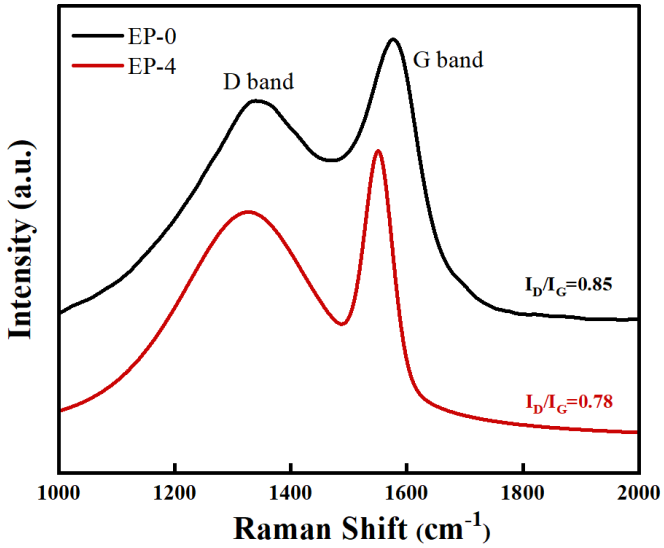


Figure. 9 Raman spectra of the residue of EP-0 and EP-4

3.9 DMA Analysis of Epoxy Resin Composites

The DMA results are shown in Figure 10. From the storage modulus (E′) curve in Figure 10 (a), it can be seen that in the glassy state region, the modulus of EP-4 is higher than that of EP-0. For example, at 50°C, the E′ of EP-0 is approximately 3.6 GPa, while that of EP-4 rises to 4.9 GPa, indicating that its resistance to elastic deformation is enhanced at low temperatures. This increase may be related to the interaction between the [CMMIm][H_2PO_4] molecules and the epoxy resin network. The polar imidazoline and amide groups can interact with the matrix through hydrogen bonds and electrostatic forces, thereby facilitating more effective stress transfer within the network. When the temperature approaches the glass transition zone, both samples' E′ drop sharply due to the increased activity of the polymer chain segments.

The tan δ curve in Figure 10 (b) shows that after adding [CMMIm][H_2PO_4], the

relaxation peak undergoes a significant shift. The peak temperature decreases from approximately 162°C of EP-0 to 131°C of EP-4, a drop of about 31°C. The lower glass transition temperature indicates an enhanced mobility of the segmental structure in the modified network, which may be attributed to the plasticizing effect of the ionic liquid and the changes in the local network structure. At the same time, the maximum tan δ value increases from approximately 0.66 to 1.04, reflecting an improvement in the viscoelastic energy dissipation capacity. These results suggest that [CMMIm][H_2PO_4] has changed the dynamic mechanical behavior of the epoxy resin network in two different ways: on the one hand, it increases the glassy state modulus, and on the other hand, it promotes the relaxation of the segmental structure at high temperatures. This enhanced damping performance may also help achieve more effective stress relaxation and energy dissipation under mechanical loads.

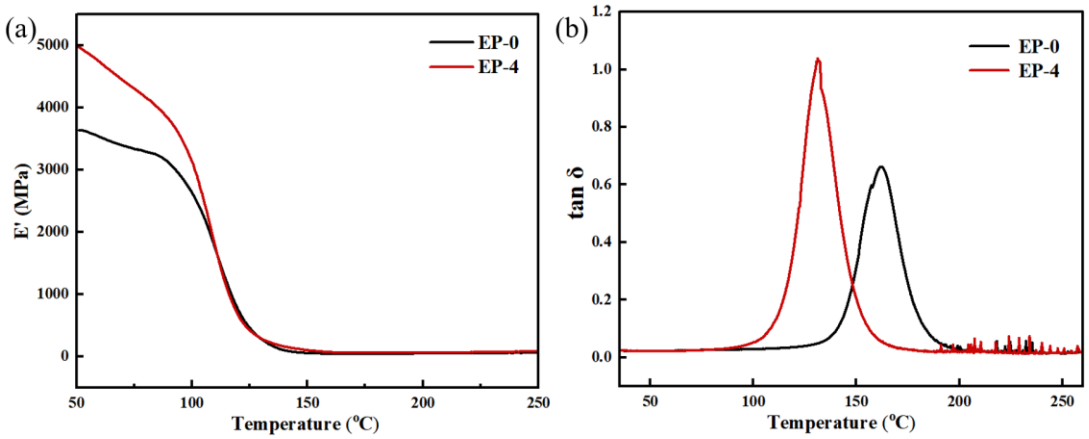


Figure.10 DMA analysis of epoxy resin composites. (a) storage modulus (E′) (b) loss factor (tan δ)

3.10 Mechanical Properties of Epoxy Resin Composites

The influence of [CMMIm][H_2PO_4] on the mechanical properties of epoxy resin was evaluated by tensile, flexural, and impact tests, and the results are presented in Figure 11. All three properties improve with increasing [CMMIm][H_2PO_4] content. The tensile strength increases from 58.65 MPa for EP-0 to approximately 73.91 MPa for EP-4, corresponding to an increase of about 26%. A similar trend is observed for the flexural modulus, which rises from 2575.90 to 3522.38 MPa, an improvement of about 37%. This increase indicates greater resistance to deformation under flexural loading. More notably, the impact strength increases from approximately 9 $kJ \cdot m^{-2}$ for EP-0 to 16.75 $kJ \cdot m^{-2}$ for EP-4, representing an improvement of about 86%. Thus, the

incorporation of [CMMIm][H_2PO_4] enhances both the strength and impact resistance of the epoxy system without sacrificing stiffness.

The improved mechanical performance is likely associated with the interaction of [CMMIm][H_2PO_4] with the epoxy network. The polar imidazolium and amide groups can interact with hydroxyl and ether groups in the matrix through hydrogen bonding and ion–dipole interactions. These interactions may strengthen the cohesion of the network and facilitate stress transfer, contributing to the increases in tensile strength and flexural modulus. At the same time, the presence of [CMMIm][H_2PO_4] may alter the local network structure and provide greater segmental mobility, allowing stress to be dissipated more effectively under impact loading. This interpretation is consistent with the DMA results, where EP-4 exhibits a higher glassy-state storage modulus together with an increased tan δ peak and a lower glass-transition temperature. The combination of stronger intermolecular interactions and enhanced energy dissipation provides a possible explanation for the simultaneous improvement in stiffness, strength, and impact resistance. Together with the flame-retardancy results, these findings show that [CMMIm][H_2PO_4] improves the fire performance of epoxy resin while retaining, and in this case enhancing, its mechanical properties.

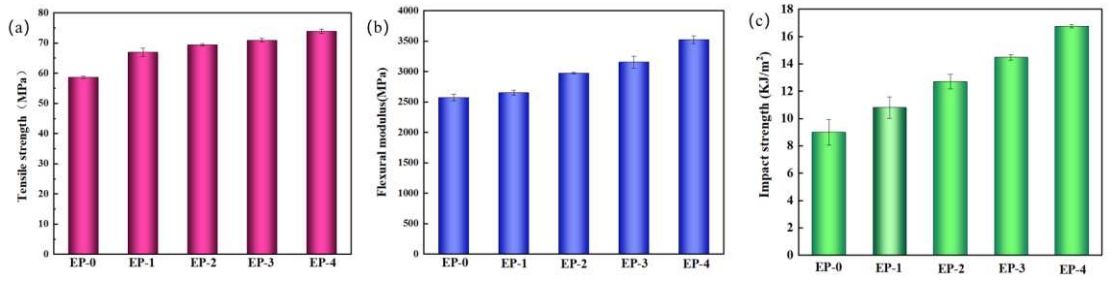


Figure 11 Mechanical property analysis EP composites. a) Tensile strength b) Flexural modulus c) Impact strength

Conclusion

In this study, the phosphorus–nitrogen-containing ionic liquid [CMMIm][H_2PO_4] was synthesized and incorporated into epoxy resin to improve its flame retardancy and mechanical properties. With increasing [CMMIm][H_2PO_4] content, the LOI increased from 20.41% for EP-0 to 30.68% for EP-4, accompanied by an increase in char residue at 800 °C from 11.64% to 16.90%. The PHRR decreased from 923.43 to 563.61 kW·m^{-}

^{2}, corresponding to a reduction of approximately 39%, while the THR decreased from 113.38 to 104.37 MJ·m^{-2}. Raman and SEM analyses further revealed that [CMMIm][H_2PO_4] favored the formation of a more ordered, compact, and continuous char layer, supporting its predominant role in condensed-phase flame retardancy.

The incorporation of [CMMIm][H_2PO_4] also altered the dynamic mechanical behavior of the epoxy network. At 50 °C, the storage modulus increased from approximately 3.6 to 4.9 GPa, whereas the glass-transition temperature decreased by about 31 °C. Together with the increase in the tan δ peak, these changes suggest higher glassy-state stiffness and greater energy dissipation during segmental relaxation. EP-4 exhibited a tensile strength of 73.91 MPa, a flexural modulus of 3522.38 MPa, and an impact strength of 16.75 kJ·m^{-2}. These results show that [CMMIm][H_2PO_4] can promote char formation and reduce heat release without compromising the mechanical performance of epoxy resin, providing a feasible approach to combining flame retardancy with improved mechanical properties.

Acknowledgements

This work was supported by the Basic Research Funds for Colleges and Universities of Liaoning Province (No. LJ212410149019) and Shandong Provincial Innovation Capacity Enhancement Project for Science and Technology-Based Small and Medium-Sized Enterprises (No. 2025TSGC087).

Data Availability Statement

All data included in this study are available upon request by contact with the corresponding author.

Conflicts of interest

The authors declare that there are no conflicts to declare.

References

[1] Jin FL, Li X, Park SJ (2015) Synthesis and application of epoxy resins: A review. J Ind Eng Chem 29:1–11. https://doi.org/10.1016/j.jiec.2015.03.026

[2] Levchik SV, Weil ED (2004) Thermal decomposition, combustion and flame-

retardancy of epoxy resins—a review of the recent literature. Polym Int 53:1901–1929. https://doi.org/10.1002/pi.1473

[3] Weil ED, Levchik SV (2004) A review of current flame retardant systems for epoxy resins. J Fire Sci 22:25–40. https://doi.org/10.1177/0734904104038107

[4] Zhi M, Yang X, Fan R et al (2022) A comprehensive review of reactive flame-retardant epoxy resin: fundamentals, recent developments, and perspectives. Polym Degrad Stab 201:109976. https://doi.org/10.1016/j.polymdegradstab.2022.109976

[5] Qiu YY, Liang B, Long JP (2025) Synthesis and application of novel imidazole-containing phosphorus–nitrogen flame retardants in epoxy resins. J Mater Sci 60:18136–18151. https://doi.org/10.1007/s10853-025-11526-w

[6] Zhang JZ, Liang JM, Long JP et al (2025) Synthesis of a novel DOPO-based ionic liquid flame retardant and its application in epoxy resin. J Mater Chem C 13:1844–1856. https://doi.org/10.1039/D4TC03681F

[7] Bifulco A, Varganici CD, Rosu L et al (2022) Recent advances in flame retardant epoxy systems containing non-reactive DOPO based phosphorus additives. Polym Degrad Stab 200:109962. https://doi.org/10.1016/j.polymdegradstab.2022.109962

[8] Sonnier R, Dumazert L, Livi S et al (2016) Flame retardancy of phosphorus-containing ionic liquid based epoxy networks. Polym Degrad Stab 134:186–193. https://doi.org/10.1016/j.polymdegradstab.2016.10.009

[9] Shi YQ, Fu T, Xu YJ et al (2018) Novel phosphorus-containing halogen-free ionic liquid toward fire safety epoxy resin with well-balanced comprehensive performance. Chem Eng J 354:208–219. https://doi.org/10.1016/j.cej.2018.08.023

[10] Meng BW, Song MH, Liang B et al (2025) Synthesis of a new flame retardant and performance study of flame retardant epoxy resin. High Perform Polym 37:32–39. https://doi.org/10.1177/09540083241302669

[11] Huo S, Wang J, Yang S et al (2019) Synthesis of a DOPO-containing imidazole curing agent and its application in reactive flame retarded epoxy resin. Polym Degrad Stab 159:79–89. https://doi.org/10.1016/j.polymdegradstab.2018.11.021

[12] Xu YJ, Shi XH, Lu JH et al (2020) Novel phosphorus-containing imidazolium as

hardener for epoxy resin aiming at controllable latent curing behavior and flame retardancy. Compos Part B Eng 184:107673. https://doi.org/10.1016/j.compositesb.2019.107673

[13] Huang R, Guo X, Ma S et al (2020) Novel phosphorus-nitrogen-containing ionic liquid modified metal-organic framework as an effective flame retardant for epoxy resin. Polymers 12:108. https://doi.org/10.3390/polym12010108

[14] Wu YS, Long JP, Liang B et al (2024) Synthesis and properties of a new halogen-free flame-retardant epoxy resin flame retardant. Pigment Resin Technol 53:62–68. https://doi.org/10.1108/PRT-01-2022-0009

[15] Ou M, Lian R, Cui J et al (2023) Co-curing preparation of flame retardant and smoke-suppressive epoxy resin with a novel phosphorus-containing ionic liquid. Chemosphere 311:137061. https://doi.org/10.1016/j.chemosphere.2022.137061

[16] Wang J, Chen X, Wang J et al (2023) High-performance, intrinsically fire-safe, single-component epoxy resins and carbon fiber reinforced epoxy composites based on two phosphorus-derived imidazoliums. Polym Degrad Stab 208:110261. https://doi.org/10.1016/j.polymdegradstab.2023.110261

[17] Wei L, Zhang X, Min F et al (2024) A flame-retardant and transparent epoxy resin based on phosphorus-containing ionic liquid and its mechanical, thermal and flame-retardant properties. React Funct Polym 197:105854. https://doi.org/10.1016/j.reactfunctpolym.2024.105854

[18] Xiao F, Shao W, Gao X et al (2024) A versatile ionic liquid enables epoxy resin with excellent fire safety and mechanical properties but ultra-low loading. Eur Polym J 219:113420. https://doi.org/10.1016/j.eurpolymj.2024.113420

[19] Long JP, Liang B, Wang ZG (2020) Enhanced mechanical properties of APP flame-retardant epoxy resin by phosphorus-modified graphene oxide. Plast Rubber Compos 49:91–100. https://doi.org/10.1080/14658011.2019.1710067

[20] Shi G, Li T, Zhou J et al (2024) Excellent flame retardant and tough epoxy thermosets with imidazolium tributyl phosphate ionic liquid. Chem Eng J 501:157613. https://doi.org/10.1016/j.cej.2024.157613

[21] Wang J, Wang J, Yang S et al (2024) Multifunctional phosphorus-containing

imidazoliums endowing one-component epoxy resins with superior thermal latency, heat resistance, mechanical properties, and fire safety. Chem Eng J 485:149852. https://doi.org/10.1016/j.cej.2024.149852

[22] Jiang L, Liang B, Long J (2024) Preparation of halogen-free flame retardant curing agent and its application in epoxy resin. High Perform Polym 36:508–518. https://doi.org/10.1177/09540083241280706

[23] Zhang C, Gong Y, Sui W et al (2025) Design and performance study of EP/CFRP based on phosphorus-containing ionic liquids: Synergistic enhancement of high strength, high toughness, and flame retardancy. Mater Today Chem 47:102812. https://doi.org/10.1016/j.mtchem.2025.102812

[24] Chen Y, Feng H, Li R et al (2025) A phosphorus-imidazole-based ionic liquid curing agent with high fire resistance and rapid curing capability, endowing epoxy resins with ultra-high toughness. Prog Org Coat 208:109522. https://doi.org/10.1016/j.porgcoat.2025.109522

[25] Huo S, Sai T, Ran S et al (2022) A hyperbranched P/N/B-containing oligomer as multifunctional flame retardant for epoxy resins. Compos Part B Eng 234:109701. https://doi.org/10.1016/j.compositesb.2022.109701